

## RESEARCH OUTPUTS / RÉSULTATS DE RECHERCHE

### Long-range resonant effects on electronic transport of nitrogen-doped carbon nanotubes

Khalfoun, Hafid; Lambin, Philippe; Henrard, Luc

*Published in:*

Physical Review. B, Condensed Matter and Materials Physics

*DOI:*

[10.1103/PhysRevB.89.045407](https://doi.org/10.1103/PhysRevB.89.045407)

*Publication date:*

2014

*Document Version*

Early version, also known as pre-print

[Link to publication](#)

*Citation for published version (HARVARD):*

Khalfoun, H, Lambin, P & Henrard, L 2014, 'Long-range resonant effects on electronic transport of nitrogen-doped carbon nanotubes', *Physical Review. B, Condensed Matter and Materials Physics*, vol. 89, no. 4, 045407. <https://doi.org/10.1103/PhysRevB.89.045407>

#### General rights

Copyright and moral rights for the publications made accessible in the public portal are retained by the authors and/or other copyright owners and it is a condition of accessing publications that users recognise and abide by the legal requirements associated with these rights.

- Users may download and print one copy of any publication from the public portal for the purpose of private study or research.
- You may not further distribute the material or use it for any profit-making activity or commercial gain
- You may freely distribute the URL identifying the publication in the public portal ?

#### Take down policy

If you believe that this document breaches copyright please contact us providing details, and we will remove access to the work immediately and investigate your claim.

**Long-range resonant effects on electronic transport of nitrogen-doped carbon nanotubes**Hafid Khalfoun,<sup>\*</sup> Philippe Lambin, and Luc Henrard*Research Center in Physics of Matter and Radiation (PMR), University of Namur, Rue de Bruxelles 61, B-5000 Namur, Belgium*

(Received 30 August 2013; revised manuscript received 1 October 2013; published 13 January 2014)

The electronic transport properties of ordered and disordered nitrogen-doped metallic carbon nanotubes with long-range correlation are studied numerically with a tight-binding model. Doping with both translational (axial) and screw symmetry are considered. In periodic defective systems, when axial doping is considered, two classes of electronic transport responses are obtained. One quantum conductance plateau settles down around the defect energy only when the period of the structure is a multiple of the Fermi wavelength  $3d_0$  ( $d_0$  being the period of the perfect armchair host nanotube), because the Bloch-like propagating modes survive. Otherwise, a conduction gap is predicted. For the screw doping configuration, the same resonant electronic transport is observed when the rotational angle fulfills one of the rotational symmetries of the perfect nanotube. Furthermore, for disordered systems, the conventional Anderson localization is partially prohibited around the defect energy for particular axial and circular random doping configurations. These conclusions are valid for both armchair and chiral metallic nanotubes and should remain true for other modifications of the nanotube by covalent or noncovalent doping.

DOI: [10.1103/PhysRevB.89.045407](https://doi.org/10.1103/PhysRevB.89.045407)

PACS number(s): 72.80.Rj, 73.63.Fg, 73.20.At, 61.48.De

**I. INTRODUCTION**

Since the pioneering work of Iijima [1] in the early 90s, carbon nanotubes (CNTs) have been studied for their unique electronic and transport properties [2]. Applications as diverse as nanoelectronics, sensors, medical imaging, flexible electronics, and photovoltaics have been proposed [3]. Poor control of the growth mechanisms has, however, curbed the development of devices with adjusted intrinsic properties, even if postsynthesis chirality sorting is improving [4]. Chemical doping and functionalization have been investigated to overcome this limitation and to tailor the electronic and structural properties of CNTs. Nitrogen (N) and boron (B) chemical substitutions are popular since they only slightly modify the atomic structure of the carbon network [5]. For example, the effects of an isolated nitrogen or boron atom on the transport properties of an armchair CNT have been examined in an early study by Choi *et al.* [6], revealing a drop of conductance from the ballistic  $2G_0$  to  $G_0$  (quantum conductance unit  $2e^2/h$ ) at the specific quasibound states energy ( $E_d$ ), located at about 0.5 eV above the Fermi level.

Many groups have reported successful strategies for the production of N-doped nanotubes [7,8]. The local electronic perturbation of a single N substitution has been observed occasionally by electron-energy-loss spectroscopy (EELS) [8] and scanning tunnel microscopy (STM) [9] but macroscopic samples are mainly characterized by a disordered distribution of defects with different atomic structures as confirmed by transport measurements [10] and photoemission spectroscopy [11]. For a precise understanding of these data, specific numerical analyses are required. For example, Latil *et al.* [12] predicted that a small amount of dopants (0.5%) with random distribution drastically affects the quantum conductance of the nanotube at the energy  $E_d$ . At this energy, the quantum resistance increases exponentially with the system length as a

clear consequence of the Anderson localization phenomenon [13]. This localization effect has been numerically simulated for substitutional chemical defects [14] and verified experimentally for different types of topological defects [15]. Similar behaviors have also been predicted for chemical functionalization [16]. Anomalous doping effects have been predicted for chemically doped carbon nanoribbons where the symmetry of the dopant position and the width of the nanoribbon strongly affect the resonant backscattering of electrons [17].

More generally, disordered systems in one-dimensional structures with chemical and/or topological defects behave as Anderson insulators at low enough temperatures [13]. However, if correlations between the defects are present, delocalized states can be obtained [18]. More precisely, as soon as the defect distribution preserves some symmetry of the original system, extended Bloch-like states can be obtained, even for infinite defective systems providing an enhancement of the transport properties for some transmission channels [19].

In the present study, we focus our attention on transport properties in periodic chemically (N) doped metallic nanotubes and we demonstrate that the ballistic properties of CNTs remains for some doping configurations, thanks to a resonant effect associated with specific symmetry of the wave function close to the Fermi level. We also show that both axial and screw periodicities give rise to such a behavior and that specific (but realistic) disorder may preserve this ballistic transport in doped metallic CNT. The reported properties are related to long-range correlation effects predicted for the electronic properties [20] and the quantum transport [21] of N-doped graphene when chemical doping affects only one of the two sublattices of graphene. At the long-range doping scale, the transport properties could be similar to the electronic transport in the multilayered diode structures [22,23].

**II. METHODS**

The electronic properties of nitrogen-doped nanotubes are described by the tight-binding model with one  $\pi$  electron per atom. Following the previous studies [2,12,16], the on-site

<sup>\*</sup>Permanent address: Laboratoire de Physique Théorique et Physique des Matériaux (LPTPM), Faculté des Sciences, Université Hassiba Benbouali, 02000 Chlef, Algérie; h.khalfoun@univ-chlef.dz

parameters of the N atom and of the neighboring C atoms are fitted to reproduce the band structure and the density of states of the *ab initio* calculations of Ref. [6]. In our works [20,24], the on-site effective parameters of the C atoms are modified around the defect up to a distance  $d_c \approx 7.5 \text{ \AA}$  along the surface of the tube, according to a Gaussian law:

$$\varepsilon(d) = \varepsilon_C - |U| \exp(-0.5d^2/\sigma^2). \quad (1)$$

$\varepsilon_C$  is the asymptotic on-site energy of carbon;  $|U|$  and  $\sigma$  are the depth and the width of the potential well induced by the nitrogen atom, respectively. By the appropriate fitting on the *ab initio* calculations, we set  $|U| \approx 6 \text{ eV}$  and  $\sigma = 15 \text{ \AA}$ .

The quantum conductance and the density of states are computed in the framework of the Green's function formalism [25,26]: The propagating media (noted  $C$ ) is embedded between two semi-infinite perfect structures as left ( $L$ ) and right ( $R$ ) leads. The corresponding Hamiltonian ( $H_C, H_L, H_R$ ) and the hopping matrices ( $h_{LC}, h_{CR}$ ) are constructed and the Green's function of the device ( $g_C$ ) is obtained from

$$g_C = (\varepsilon - H_C - \Sigma_L - \Sigma_R)^{-1}. \quad (2)$$

In this equation,  $\Sigma_L = h_{LC}^+ g_L h_{LC}$  and  $\Sigma_R = h_{RC} g_R h_{RC}^+$  are the left and right self-energies while  $g_{L,R} = (\varepsilon - H_{L,R})^{-1}$  are the Green's functions of the left and right leads, respectively. The conductance response  $G$  is obtained from

$$G = \text{Tr} \left[ \Gamma_L g_C^r \Gamma_R g_C^a \right] \frac{2e^2}{h}, \quad (3)$$

where  $\Gamma_{L,R} = i[\Sigma_{L,R}^r - \Sigma_{L,R}^a]$  are the coupling matrices at the interfaces  $C/R$  and  $C/L$ . In this formula,  $\Sigma_{L,R}^a$  and  $\Sigma_{L,R}^r$  are Hermitian conjugates. The  $r$  and  $a$  superscripts correspond to the retarded and advanced Green's functions, respectively. The density of states per spin is obtained from

$$\text{dos}(E) = -\frac{1}{\pi} \text{Im} \{ \text{Tr} [g_C(E)] \}. \quad (4)$$

$\text{Tr}$  denotes the trace of the matrix and  $\text{Im}$  is the imaginary part [25,26].

In this paper, the host system (perfect CNT) is made of supercells of size  $d = n_{\text{cell}} d_0$  ( $d_0$  the periodicity of the host nanotube), containing one nitrogen atom [Fig. 1(a)]. The parameter  $n_{\text{cell}}$  is taken large enough to ensure that the distance between dopants is larger than twice the size of the local perturbation ( $d_c$ ) of the Hamiltonian for an isolated N atom.

### III. RESULTS AND DISCUSSION

We first consider the effect of nitrogen chemical doping on the armchair (10,10) nanotubes as an archetype of metallic system with high symmetry. Axial and screw periodicity of the dopant position are investigated as well as the effect of disorder. Based on these results and on a symmetry analysis, we then extend our findings to chiral nanotubes.

#### A. Doping with axial periodicity and disorder for (10,10) nanotube

For the (10,10) nanotube,  $d_0 = 2.45 \text{ \AA}$  and the distance between two nitrogen atoms is always set larger than  $7d_0$ . In the following, we present simulations for the quantum

conductance  $G(E)/G_0$  as a function of the energy for two supercell periods with  $n_{\text{cell}}$  being a multiple of 3 or not, i.e.,  $n_{\text{cell}} = 15$  and  $n_{\text{cell}} = 14$ , corresponding to defect concentrations of 0.166% and 0.178%, respectively.

#### 1. The effect of the axial periodicity

The effect of  $n$  dopants (i.e., number of doped supercells between the perfect electrodes) separated by the distance  $d$  is shown for several values of  $n$  [Schematic view on Fig. 1(a). Figures 1(b) and 1(c) correspond to  $d = 14d_0$  and  $d = 15d_0$  respectively]. For  $n = 1$  (isolated defect, dashed line), we recover the *ab initio* results of Ref. [6], i.e., a unique conductance dip ( $G = 1G_0$ ) at  $E_d = 0.54 \text{ eV}$ , the energy of the quasibound states of the electrons localized around the nitrogen atom. The presence of this quasibound state is responsible for the backscattering of electrons in one of the two conduction channels because of the symmetry reduction of the system in the presence of the defect [6].

When two dopant atoms are considered ( $n = 2$ , red curve), distinct responses around  $E_d$  are obtained for  $d = 14d_0$  [ $G(E_d) = 0$ ] and  $d = 15d_0$  [ $G(E_d) = 1G_0$ ]. The conductance displays clear local maxima (see arrows) and minima for  $d = 15d_0$ . This behavior can be explained by the fact that the Fermi wave vector  $k_F = 2\pi/3d_0$  of an undoped armchair nanotube is associated with a Fermi wavelength of  $3d_0$ . Each conductance maximum corresponds to constructive interferences between defect-induced quasibound states inside the quantum cavities as delimited by the dopant positions. The corresponding conductance peaks can exist only if the size of the supercell is an integer multiple of the Fermi wavelength (as for  $n_{\text{cell}} = 15$ ) and the transmission of the electrons behaves similarly as in resonant multiple-barrier diodes [22,23]. In the other case, when  $n_{\text{cell}}$  is not a multiple of 3, the distance between the defects is no more related to the Fermi wavelength and two consecutive defects incoherently backscatter the propagating waves of the two conductive channels. Consequently, the conductance drops to zero at  $E_d$  and no resonant conduction is observed anymore around this energy.

When the number of nitrogen atoms  $n$  increases further, the conductance  $G$  remains around  $1G_0$  for  $15d_0$  even when  $n = 10$  and the maxima of  $G$  are transformed into multiple oscillations. The splitting of the maxima is due to the coupling between quasibound states inside the adjacent quantum boxes as in the quantum superlattices [23]. The value of the conductance plateau around  $E_d$  is slightly smaller than  $G_0$  because beside the resonance effect described above, the second channel of conduction is also affected by the chemical disorder induced by the substitution.

The band structure of infinite periodic systems gives us more insight on the behavior of the conductance curves [Figs. 1(d) and 1(e)]. For  $d = 15d_0$ , the presence of the dopant lifts the twofold degeneracy. However, one of the folded electronic bands remains nearly unaffected as it can be observed by comparison with the perfect nanotube [Fig. 1(g)]. Consequently, no electronic gap opens and one channel of conduction remains unaffected. However, the opening of pseudogaps at  $k = 0$  or  $k = \pi/d$  is responsible for the drop of conductance to  $G = 1G_0$  at those energies. As for the

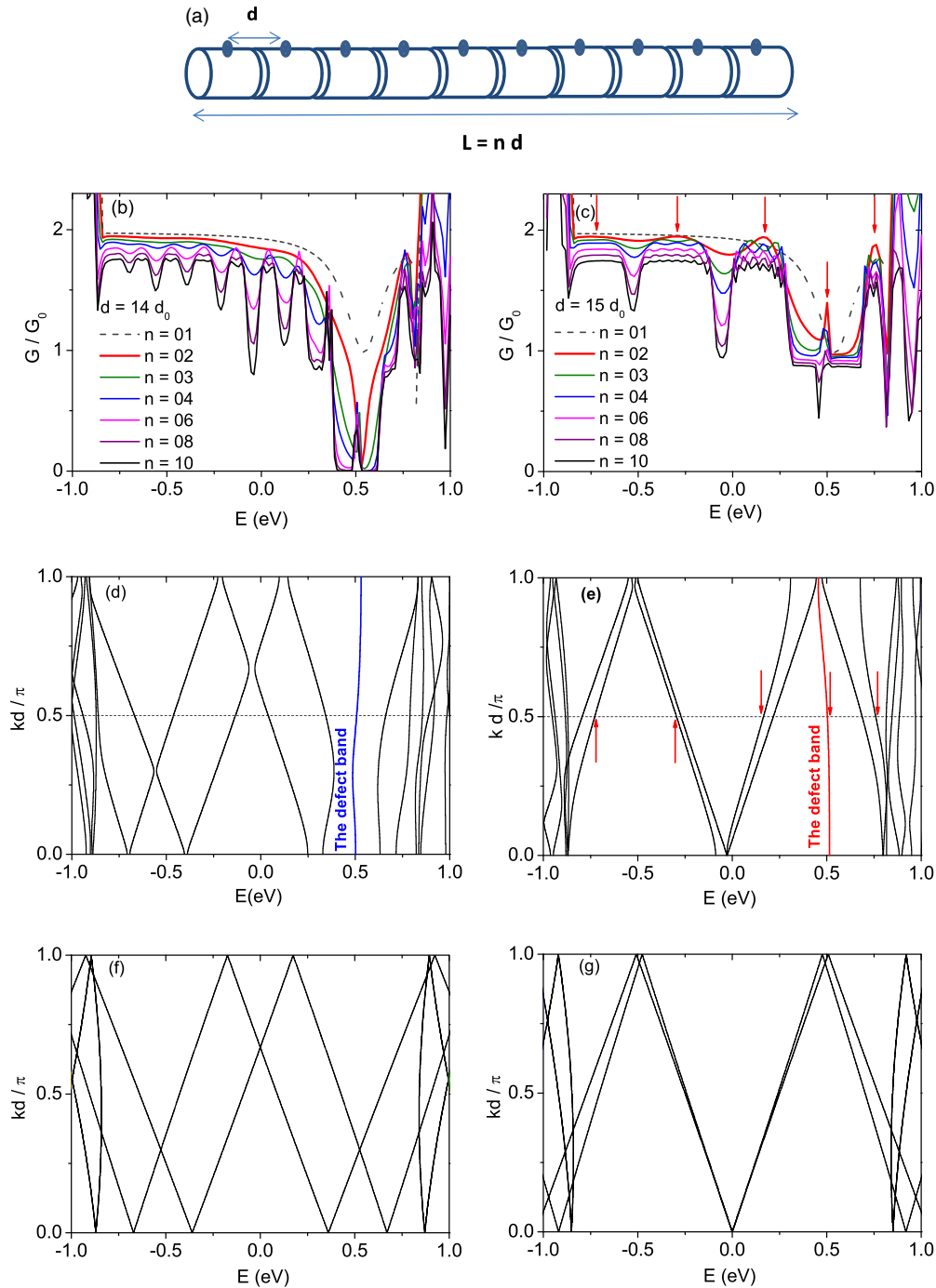


FIG. 1. (Color online) (a) Schematic representation of an ordered defective nanotube.  $d$  is the unit cell length while  $L = nd$  is the system length and  $n$  is an integer. Conductance curves of a (10,10) CNT with distance between the dopants (b)  $d = 14d_0$  and (c)  $d = 15d_0$  ( $1 \leq n \leq 10$ , from top to bottom).  $d_0 = 2.46 \text{ \AA}$  is the periodicity of the perfect (10, 10) CNT and  $G_0$  is the quantum conductance. The tight-binding band structure of infinite systems for (d)  $d = 14d_0$  and (e)  $d = 15d_0$ . The Fermi level is located at  $E = -0.048 \text{ eV}$  and  $E = -0.025 \text{ eV}$ , respectively. The arrows indicate the principal maxima of the quantum conductance related to  $n = 2$ . (f) and (g) The tight-binding band structure for the infinite perfect systems.

wave functions, a surprising quasiperiodic oscillation with wavelength equal to the Fermi wavelength  $3d_0$  is reproduced at the energies of the  $1G_0$  conductance plateau around  $E_d$  (not shown in the paper). This particular length comes from a beating effect between the corresponding  $\pi$  and  $\pi^*$  states at  $E_d$  of the perfect armchair CNT.

For  $d \neq 3nd_0$ , band crossings are much more numerous in the folded Brillouin zone due to lower symmetry [Fig. 1(f)]. True electron gaps appear at the energy of each band crossing with a particularly large one around the band defect energy ( $E_d$ ) [see Fig. 1(d)]. Much more minima then occur in the conductance curve. We also note that the presence of a

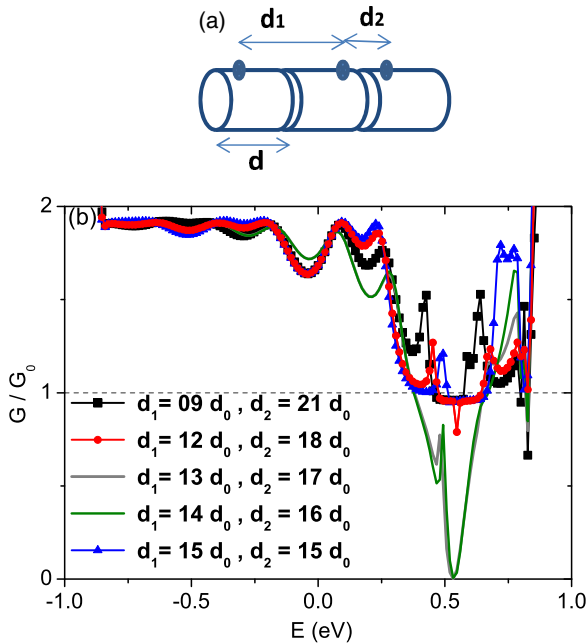


FIG. 2. (Color online) Conductance of a (10, 10) CNT with three nitrogen atoms, separated by distances  $d_1$  and  $d_2$ . The total distance  $d_1 + d_2$  is kept constant at  $30d_0$  ( $d_0 = 2.46 \text{ \AA}$ ).

nondispersive band at  $E_d$  is associated with localized states. This band does not participate in the electron transport when  $d > d_c$ .

## 2. The effect of the axial disorder

We now consider disorder by introducing randomness in the axial position of the dopant atom inside each supercell. The distance between consecutive dopant atoms  $d_{N-N}$  is then modified, but not the average distance between them (or the total size of the system)

In Fig. 2, the effect of two successive cavities with different sizes  $d_1$  and  $d_2$  is shown for constant  $d_1 + d_2 = 30d_0$ . The  $G_0$  conductance plateau is preserved around  $E_d$  when  $d_1$  and  $d_2$  are both multiples of  $3d_0$  even if they are different. This clearly indicates that one conduction channel remains open even if the dopants are not periodically positioned along the tube axis as long as the distance between them is related to the periodicity of the wave function.

We examine now the cavity effect for longer systems [ $n = 8$ ; see Fig. 3(a) for a schematic representation]. In Fig. 3(b), the averaged electronic density of states and the transmission coefficient are presented for a periodic arrangement of the nitrogen dopants (black curve), for a system with random axial position of the nitrogen dopants (red curve), and for a system with a pseudorandom axial position such that each  $d_{N-N}$  is always a multiple of  $3d_0$  (blue curve). For totally random  $d_{N-N}$ , the propagating electron waves are fully backscattered around  $E_d$  (red curve) and no conductivity is observed anymore despite the large amount of states located around  $E_d$  (see the density of states, red curve). The propagating media behave like an Anderson insulator in this energy domain. When  $d_{N-N}$  is a multiple of  $3d_0$  (blue curve), the  $1G_0$  conductance plateau remains around  $E_d$ , similarly as in the periodic case (black curve). High density of states is also observed in the last two cases

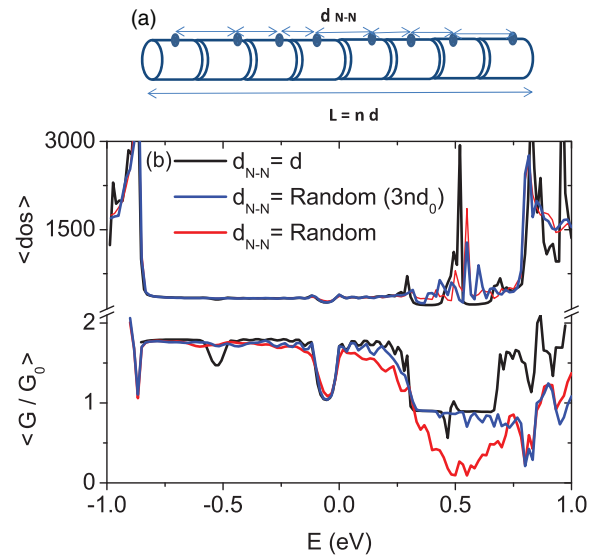


FIG. 3. (Color online) (a) Schematic representation of the random axial disorder ( $n = 8$ ). (b) Averaged conductance  $\langle G \rangle$  and averaged density of states  $\langle \text{dos} \rangle$  of a nitrogen-doped CNT for different distributions of  $d_{N-N}$ :  $d_{N-N} = d = 15d_0$  corresponds to ordered defective case (black curve) while for the disordered configurations,  $d_{N-N}$  is a random multiple of  $3d_0$  (blue curve) or  $d_{N-N}$  takes totally random values (red curve).

associated with the Anderson localization process for one of the conduction channels while the other channel remains open. A difference between the periodic configuration and the random  $3nd_0$  is obviously observed at other energies, i.e.,  $E \approx -0.5 \text{ eV}$  when peculiar quantum box behavior occurs.

## B. Screw periodicity and circular disorder for (10,10) nanotube

In this section, we study the conductance of doped nanotubes with a screw periodicity of the defect positions. Both ordered and disordered cases will be examined for the same systems characterized by  $d = 15d_0$  and  $n = 8$  supercells.

A screw operator  $S(d, \vartheta)$  is defined by a translation  $d$  and a rotation  $\vartheta$ . For a (10,10) nanotube, because of the periodicity  $d_0$  and the tenfold rotational symmetry, only four out of the 40 atoms of the unit cell are sufficient to describe the system (we ignore here mirror and axial symmetries which can reduce to 2 the number of inequivalent atoms). The screw operator  $S(md_0, k2\pi/10)$  projects one atom on an equivalent position of the system. The four atoms are named A, B, C, and D [see Fig. 4(b)]. The axial periodicity and disorder studied previously correspond to  $m = 3n$  and  $k = 0$ . We investigate here the robustness of the previous conclusions for different values of  $k$  and for rotational disorder while keeping  $m = 3n$ .

From Fig. 4(c), we observe that for any integer value of  $k$  [ $k = 1$  (red curve) and  $k = 5$  (blue curve) for example], the quantum conductance responses are almost indistinguishable from the axial periodic ordered case ( $k = 0$ , black curve). This means that the  $1G_0$  conductance plateau is preserved around  $E_d$  and that the resonant conduction behavior (quantum box effect) still takes place. We explain this behavior by the symmetry of the (10,10) tube. Indeed, the electron wave function that contributes to the transport of one quantum of

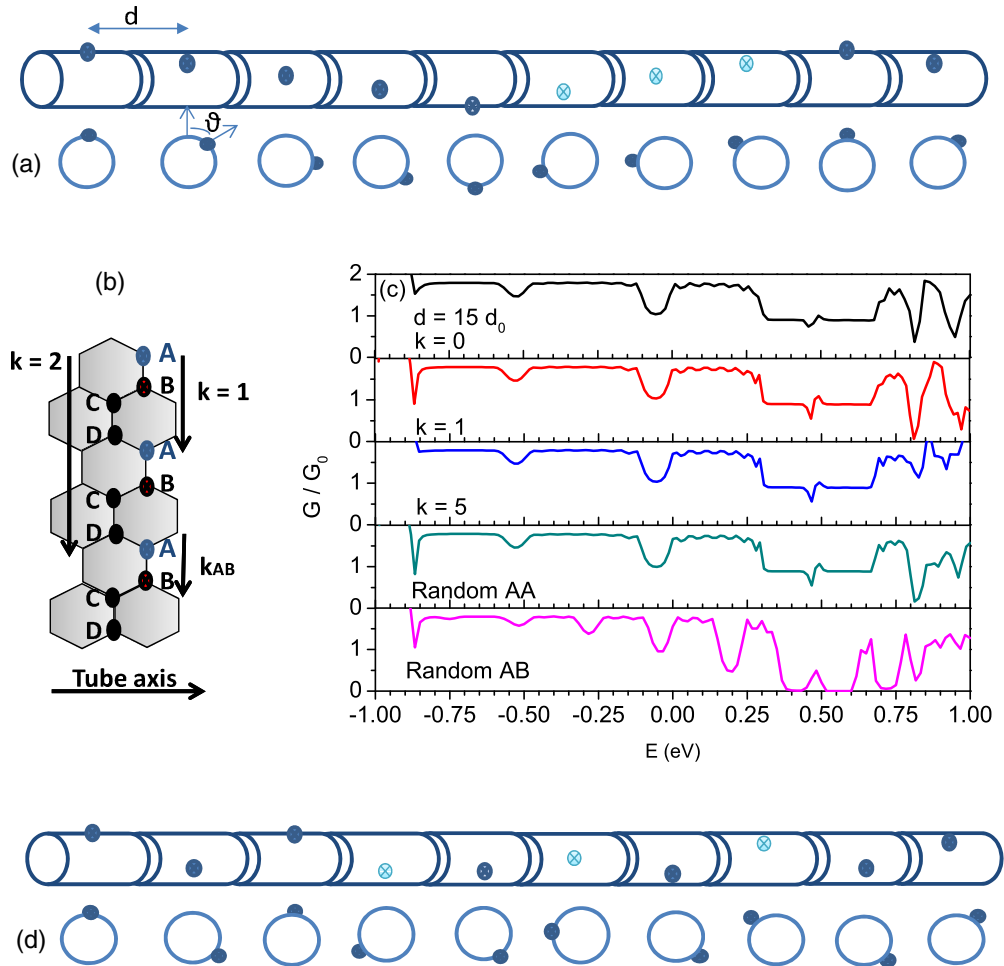


FIG. 4. (Color online) Schematic representation of (a) the screw configuration  $S(d, \vartheta)$  and (d) the random screw configuration. (b) Part of one (unrolled) unit cell of the (10, 10) nanotube. The four atoms A, B, C, D and the effect of the rotation  $\vartheta = k2\pi/10$  for  $k = 1$  and  $k = 2$  are represented. (c) The conductance responses (from top to bottom) for the ordered case ( $k = 0$ ), the screw periodic configurations ( $k = 1$  and  $k = 5$ ), the random screw configuration AA (integer random values for  $k$ ), and the random screw configuration AB ( $k_{AB}$  is a translation vector from A to B sites).

conductance for one single nitrogen substitution not only has a  $3d_0$  oscillation periodicity but also preserves a reminiscence of the tenfold rotational symmetry. Consequently, the rotation by an angle  $k2\pi/10$  of the position of the nitrogen atom does not modify the transport properties of the system.

Furthermore, the transport properties are not modified if we introduce a circular disorder in the doping scheme as long as the dopants remain on the same A sublattice. Such disorder is here analyzed by considering that two successive nitrogen positions are rotated by  $\vartheta = k2\pi/10$  ( $k$  being a random integer) with an axial distance  $d_{N-N}$  still fixed ( $d_{N-N} = 15d_0$ ) [see Fig. 4(c) for random  $k$ ; i.e., random AA configuration].

Other rotational disorders (no longer multiples of  $2\pi/10$ ) close the remaining conduction channel and lead to an electronic transport gap around  $E_d$ . For example, on the bottom panel of Fig. 4(c), we see that a random distribution of nitrogen defects on A and B type positions, while preserving the  $d = 15d_0$  periodicity, leads a conductance curve typical of uncorrelated disorder.

### C. Combined axial and circular disorders for (10,10) nanotube

In order to show the robustness of the electronic conductivity of doped carbon nanotubes for more general disorders, we have mixed circular and axial disorders. In Fig. 5(b), we show the average density of states and transport properties for nitrogen-doped CNT when a pseudorandom distance between the N atoms is considered ( $d = 3md_0$  with  $m$  a random integer). In the first case (black curve), we apply a circular disorder  $\vartheta = k2\pi/10$ , with  $k$  a random integer. We observe that the  $1G_0$  conductance plateau is preserved around  $E_d$ . However, if a totally random rotation is taken between successive N atoms (red curve), this plateau disappears.

### D. Chiral nanotubes

We now extend to metallic chiral nanotubes the previous investigations on the Bloch-like behavior of electronic transport in disordered chemically doped systems. It is well known that chiral nanotubes could have large translational unit cells and can be described by screw operators [27]. For example, the (15,6) CNT has a translational periodicity of  $d_0 = \sqrt{13}a_0$  with

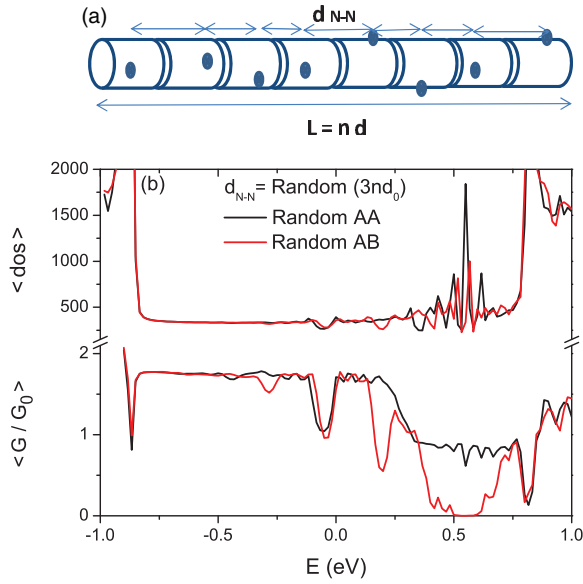


FIG. 5. (Color online) (a) Schematic representation of the combined random screw configuration with the axial translation. (b) The averaged conductance  $\langle G \rangle$  and density of states  $\langle \text{dos} \rangle$  of doped (10,10) CNT for combined axial and circular disorders (see text).

78 hexagons, a chiral angle  $\Theta = 16^\circ$ , and a threefold rotation axis. In the reciprocal space of the associated graphene plane (of the unrolled nanotube), the axial direction of the tube makes

an angle of  $\Theta' = 30^\circ - \Theta = 14^\circ$  with the  $\Gamma$ - $K$  direction of graphene [Fig. 6(b)]. The condition to have a distance between successive dopant  $d = 3nd_0$  in the graphene plane becomes  $z = 3nd_0 \cos(\Theta')$  when measured along the axial direction. In fact, as illustrated in Fig. 6(c) for the (15,6) CNT, the conductance curve is very similar to that already found in (10,10) for  $d = 3nd_0$ : The plateau around  $E_d$  is preserved even when  $d_1 \neq d_2$  provided both  $d_1$  and  $d_2$  are integer multiples of  $3d_0$ . Otherwise a conductance gap around  $E_d$  is observed.

The rotational disorder has also been examined for the nitrogen-doped (15,6) CNT. In Fig. 6(d), we see that a rotation  $\Delta\Phi$  around the tube axis of the second (central) nitrogen atom does not qualitatively modify the conductance curves if it corresponds to the threefold axis of the nanotube ( $\Delta\Phi = 0^\circ, 120^\circ, \text{ and } 240^\circ$ ), while other rotation angles (with no change of the  $z$  position) open a conduction gap.

Another rotational disorder has been investigated. Indeed, following our conclusions on the armchair tubes and from the measurement of the distance along the  $\Gamma$ - $K$  direction in the chiral tube, we explore the effect of a displacement of the defect position in a direction perpendicular to this  $\Gamma$ - $K$  direction [see Fig. 6(b)]. In this direction, a displacement of the defect along the helix is equivalent to a rotation around the circumference of the tube for an armchair CNT and can be described by the four atomic positions (A, B, C, D), repeated  $i$  times according to the translational vector  $k_i$  [as described for armchair tube in Fig. 4(b)]. Figure 6(e) shows that such screw operation for the disorder pattern does not close the conduction channel.

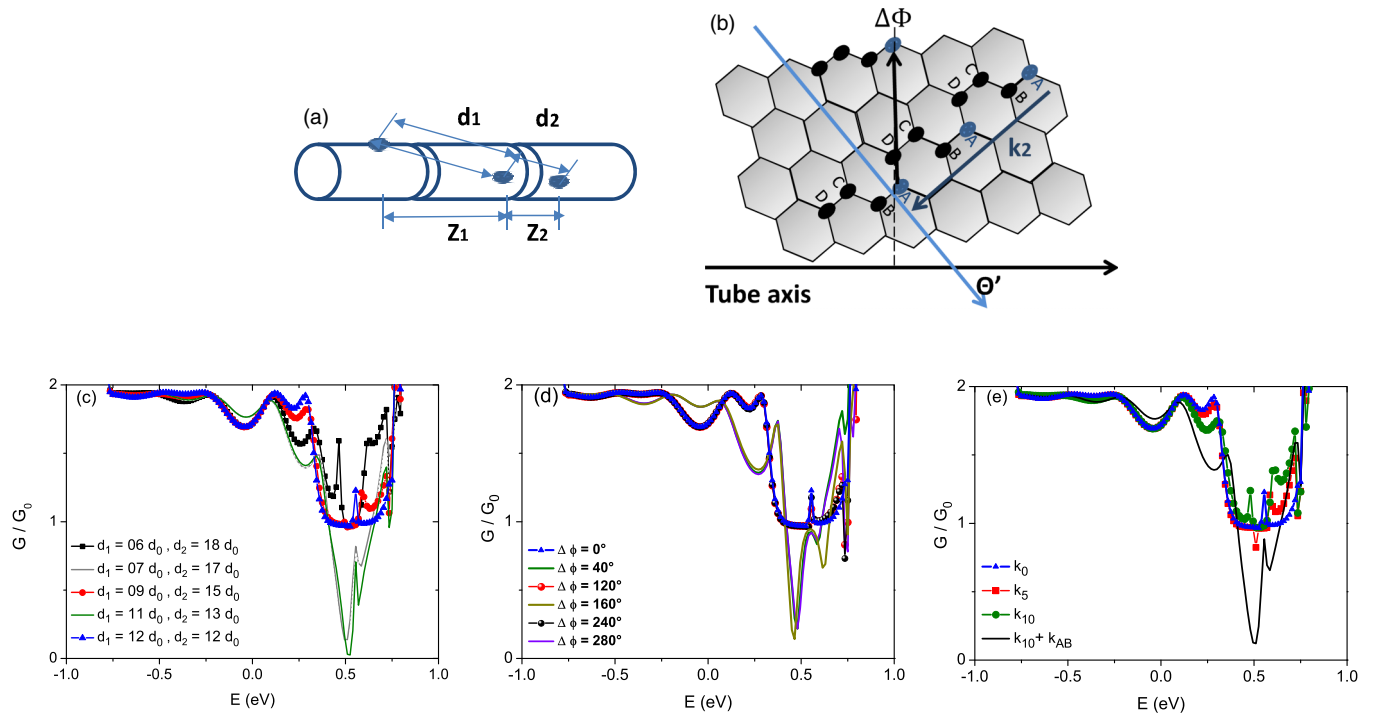


FIG. 6. (Color online) (a) Schematic representation of a nanotube with three nitrogen atoms separated by the distances  $d_1$  and  $d_2$  along the nanotube (or by axial distances  $z_1$  and  $z_2$ ). (b) The rotational and screw defect configurations as defined perpendicularly from the tube axis and the helix direction, respectively.  $\Delta\Phi$  is the rotational angle of the tube and  $k_2$  is a translational vector, respectively. Conductance for the (15,6) nanotube when (c) the total distance  $d_1 + d_2$  is kept constant and equal to  $24d_0$  along the direction. (d) the central defect undergoes a circumferential translation according to the rotational angle  $\Delta\Phi$  from its initial position  $d_1 = 12d_0$  ( $\Delta\Phi = 0^\circ$ ). (e) The central defect undergoes a translation  $k_i$  perpendicular to the helical direction from its initial position  $d_1 = 12d_0$  (site labeled A corresponding to  $k_0 = 0$ ) to any other site A (the subscript  $i$  taking an integer value).  $k_{AB}$  is a translation vector from A to B sites.

We conclude that the resonant (or Bloch-like) transport is also present for chiral nanotubes when the distance between the defects remains proportional to the Fermi wavelength of graphene. However the chiral angle has to be correctly taken into account to understand the absence of Anderson localization. Two kinds of rotational disorders keep one conduction channel open: a true rotation (if the chiral NT admits one) and a screw operation.

#### IV. CONCLUSION

The electronic transport properties of nitrogen chemically doped nanotubes with long-range correlation have been studied using the Green's function formalism in the framework of the tight-binding approach with effective parameters. Resonant conduction behavior and ballistic transport have been demonstrated for particular positions of the dopant: a specific distance between the dopants (i.e., multiple of  $3d_0$ ) and a specific rotational angle  $\vartheta$  related to the symmetry of the tube. These doping patterns have been shown to preserve the Bloch-like transport properties and then to avoid Anderson localization around  $E_d$ . Indeed, the conductance response is almost unchanged because one of the two conductance channels remains open for symmetry reasons. This property remains true for both armchair and chiral nanotubes. The present results somehow reproduce the electronic properties of periodic N-doped graphene [20]: opening of a gap for a  $n \times n$  supercell when  $n$  is not a multiple of 3 while no gap opens

otherwise. Further studies on electronic transport properties for longer systems and for two-dimensional structures at the mesoscopic scale are under investigation.

The present conclusion has been drawn for specific chemical substitution of carbon atoms by nitrogen. It should remain qualitatively valid for other local modifications of the nanotube, by other chemical species, by covalent or noncovalent functionalization. The energy of the quasibound states will depend on the specific local modification but not the general conclusions based on the symmetry of the quasibound states. The method used for postsynthesis sorting of the CNT by DNA wrapping [4] presents all the characteristics of local modification of the CNT with a screw periodicity. Resonant conductivity could be achieved in this case, which should be worth investigating. Other experimental confirmations of the resonant electronic waves for correlated defects could also come from STM measurements as demonstrated recently in Ref. [9].

#### ACKNOWLEDGMENTS

The authors acknowledge Professor Jean-Christophe Charlier from U. C. Louvain, Belgium, for constructive discussions. This research used resources of the "Plateforme Technologique de Calcul Intensif (PTCI) located at the University of Namur, Belgium, which is supported by the F.R.S.-FNRS. The PTCI is a member of the "Consortium des Équipements de Calcul Intensif (CÉCI)." This work is supported by the FSR -FNRS under Project No. 4 9137 E1.

- 
- [1] S. Iijima, *Nature* **354**, 56 (1991).
  - [2] J. C. Charlier, X. Blaise, and S. Roche, *Rev. Mod. Phys.* **79**, 677 (2007); S. M. M. Dubois, Z. Zanolli, X. Declerck, and J. C. Charlier, *Eur. Phys. J. B* **72**, 1 (2009).
  - [3] A. Jorio, G. Dresselhaus, and M. S. Dresselhaus, *Carbon Nanotubes: Advanced Topics in the Synthesis, Structure and Applications* (Springer, Berlin, 2008).
  - [4] X. Tu, S. Monohar, A. Jagota, and M. Zheng, *Nature* **460**, 250 (2009).
  - [5] B. Zheng, P. Hermet, and L. Henrard, *ACS Nano* **4**, 4165 (2010).
  - [6] H. J. Choi, J. Ihm, S. G. Louie, and M. L. Cohen, *Phys. Rev. Lett.* **84**, 2917 (2000).
  - [7] M. Glerup, J. Steinmetz, D. Samaille, O. Stephan, S. Enouz, A. Loiseau, S. Roth, and P. Bernier, *Chem. Phys. Lett.* **387**, 193 (2004).
  - [8] H. Lin, J. Lagoute, C. Chacon, R. Arenal, O. Stephan, V. Repain, Y. Girard, S. Enouz, L. Bresson, S. Rousset, and A. Loiseau, *Phys. Status Solidi B* **245**, 1986 (2008).
  - [9] Y. Tison, H. Lin, J. Lagoute, V. Repain, C. Chacon, Y. Girard, S. Rousset, L. Henrard, B. Zheng, T. Susi, E. I. Kauppinen, F. Ducastelle, and A. Loiseau, *ACS Nano* **7**, 7219 (2013).
  - [10] P. Ayala, R. Arenal, A. Loiseau, A. Rubio, and T. Pichler, *Rev. Mod. Phys.* **82**, 1843 (2010).
  - [11] V. Kristic, G. L. J. A. Rikken, P. Bernier, S. Roth, and M. Glerup, *Europhys. Lett.* **77**, 37001 (2007).
  - [12] S. Latil, S. Roche, D. Mayou, and J.-C. Charlier, *Phys. Rev. Lett.* **92**, 256805 (2004); S. Latil, S. Roche, and J.-C. Charlier, *Nano Lett.* **5**, 2216 (2005).
  - [13] P. W. Anderson, D. J. Thouless, E. Abrahams, and D. S. Fisher, *Phys. Rev. B* **22**, 3519 (1980); E. Abrahams, P. W. Anderson, D. C. Licciardello, and T. V. Ramakrishnan, *Phys. Rev. Lett.* **42**, 673 (1979).
  - [14] C. Adessi, S. Roche, and X. Blase, *Phys. Rev. B* **73**, 125414 (2006); R. Avriller, S. Roche, F. Triozon, X. Blase, and S. Latil, *Mod. Phys. Lett. B* **21**, 1955 (2007).
  - [15] C. Gomez Navarro, P. J. de Pablo, J. Gomez-Herrero, B. Biel, F. J. Garcia-Vidal, A. Rubio, and F. Flores, *Nat. Mater.* **4**, 534 (2005); F. Flores, B. Biel, A. Rubio, F. J. Garcia-Vidal, C. Gomez-Navarro, P. de Pablo, and J. Gomez-Herrero, *J. Phys.: Condens. Matter* **20**, 304211 (2008); B. Biel, F. J. Garcia-Vidal, A. Rubio, and F. Flores, *ibid.* **20**, 294214 (2008).
  - [16] A. López-Bezanilla, F. Triozon, S. Latil, X. Blase, and S. Roche, *Nano Lett.* **9**, 940 (2009).
  - [17] B. Biel, X. Blase, F. Triozon, and S. Roche, *Phys. Rev. Lett.* **102**, 096803 (2009); B. Biel, F. Triozon, X. Blase, and S. Roche, *Nano Lett.* **9**, 2725 (2009).
  - [18] F. M. Izrailev, A. A. Krokhin, and N. M. Makarov, *Phys. Rep.* **512**, 125 (2012).
  - [19] D. H. Dunlap, H.-L. Wu, and P. W. Phillips, *Phys. Rev. Lett.* **65**, 88 (1990); P. Phillips and H.-L. Wu, *Science* **252**, 1805 (1991); F. M. Izrailev and A. A. Krokhin, *Phys. Rev. Lett.* **82**, 4062 (1999); F. M. Izrailev, A. A. Krokhin, and S. E. Ulloa, *Phys. Rev. B* **63**, 041102 (2001).
  - [20] P. Lambin, H. Amara, F. Ducastelle, and L. Henrard, *Phys. Rev. B* **86**, 045448 (2012).
  - [21] A. Lherbier, A. R. Botello-Méndez, and J.-C. Charlier, *Nano Lett.* **13**, 1446 (2013).

- [22] L. Esaki and R. Tsu, *IBM J. Res. Dev.* **14**, 61 (1970).
- [23] X.-W. Liu and A. P. Stamp, *Phys. Rev. B* **47**, 16605 (1993).
- [24] H. Khalfoun, P. Hermet, L. Henrard, and S. Latil, *Phys. Rev. B* **81**, 193411 (2010).
- [25] S. Datta, *Electronic Transport in Mesoscopic Systems* (Cambridge University Press, Cambridge, 1995).
- [26] M. Buongiorno Nardelli, *Phys. Rev. B* **60**, 7828 (1999).
- [27] M. S. Dresselhaus, G. Dresselhaus, and P. C. Eklund, *Sciences of Fullerenes and Carbon Nanotubes* (Academic, New York, 1996).